Digital Object Identifier (DOI): 10.1109/APEC.2014.6803608

Applied Power Electronics Conference and Exposition (APEC), 2014 IEEE

An active damper to suppress multiple resonances with unknown frequencies

Xiongfei Wang
Frede Blaabjerg
Marco Liserre

Suggested Citation

X. Wang, F. Blaabjerg and M. Liserre, "An active damper to suppress multiple resonances with unknown frequencies," *2014 IEEE Applied Power Electronics Conference and Exposition - APEC 2014*, Fort Worth, TX, 2014, pp. 2184-2191.

An Active Damper for Suppressing Multiple Resonances with Unknown Frequencies

Xiongfei Wang, Frede Blaabjerg, and Marco Liserre
Department of Energy Technology, Aalborg University, Aalborg, Denmark
xwa@et.aau.dk, fbl@et.aau.dk, mli@et.aau.dk

***Abstract*—The increasing use of power electronics devices tends to aggravate high-frequency harmonics in the power system and trigger resonances across a wide frequency range. This paper presents an active damper to suppress multiple resonances with unknown frequencies. The active damper is realized by a high-bandwidth power converter that can dynamically control the voltages at the resonance frequencies of concern. A cascaded adaptive notch filter structure is proposed for the detection of resonance frequencies, which thus enables the active damper to separately suppress the different resonances. The performance of the active damper is validated by applying it to suppress the resonances in a grid-connected inverter through a long power cable. The results show that the active damper can become a promising way to stabilize the future power electronics based power systems.**

I. INTRODUCTION

There is a growing demand on the use of power electronics converters to connect renewable energy sources and industrial drives to electric power grid [1]. Power electronics is enabling the development of the energy-efficient, sustainable and smart power systems [2]. With the increasing use of high-frequency switching power converters, the power system characteristics have gradually been changed. The high-frequency harmonics tend to be more apparent and the system damping is reduced due to the small time constants of converters. These wideband frequency harmonics may interfere with other devices in the power system and trigger resonances across a wide frequency range [3]. To reduce the high-frequency switching ripples, the high-order power filters are widely adopted for converters [4]. However, the shunt capacitors in these filters may also lead to resonances, which tend to be more severe when the multiple converters are interconnected [5]-[7]. Also, the use of power cables in renewable power plants may further aggravate the resonance propagation due to the parasitic capacitances [8].

To address the wideband harmonics and resonances in the future power electronics based power system, the extensive research works have been made, which either introduce the additional control loop for power converters [9]-[11], or add the passive damping circuit into the filters [12]-[14]. However, most of them are either limited by the dynamic behavior of converters or sensitive to the uncertainties of power system conditions. To overcome these drawbacks, an active damper concept that is based on a high-bandwidth power converter is recently introduced [15]. As opposed to reshaping the terminal behavior of converters, the active damper controls the resonant voltages at the Point of Common Coupling (PCC) to terminate the resonance propagation. The active damper can operate in a similar way to the Resistive-Active Power Filter (R-APF) by synthesizing the virtual damping resistances at the resonance frequencies [16]. But instead of compensating the low-order harmonic distortions as in the R-APF, the active damper only works for the resonances, thus allowing a low power design and high control bandwidth. Also, the detection of resonance frequencies becomes more important for the active damper. In [15], only the detection and prevention of single resonance is attained, whereas the wideband harmonics in real cases may trigger double or multiple resonances [17].

This paper presents an active damper that can suppress the multiple resonances with unknown frequencies. A cascaded Adaptive Notch Filter (ANF) structure based on the multiple ANFs and Frequency-Locked Loops (FLLs) is proposed to detect the resonance frequencies. Thus, the active damper is enabled to selectively control the resonant voltages by means of multiple frequency adaptive resonant voltage controllers. The performance of the active damper is validated by applying it for a three-phase grid-connected inverter through the long power cable. The results show that active damper provides an effective way to suppress the resonance propagation along the power cable and the output *LCL*-filter of inverter.

II. ACTIVE DAMPER

A. System Configuration

Fig. 1 illustrates a simplified one-line diagram of an active damper for a three-phase voltage source inverter connected to the grid via a long power cable. The grid-side inductor current (i_g) of the *LCL*-filter is controlled for the inverter, such that no additional damping is needed when the *LCL*-filter resonance frequency is higher than the one-sixth of the control sampling frequency [18]. However, the variation of grid impedance and

This work was supported by European Research Council (ERC) under the European Union's Seventh Framework Program (FP/2007-2013)/ERC Grant Agreement [321149-Harmony].

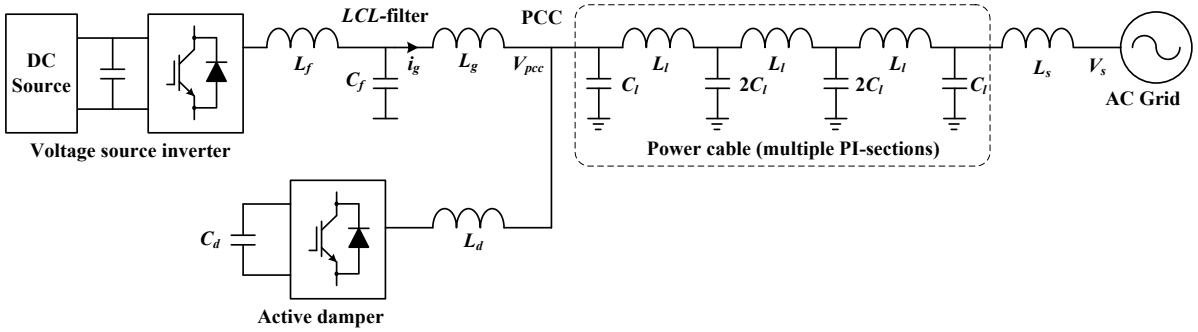

Fig. 1. Simplified one-line diagram of an active damper for a grid-connected voltage source inverter through a long power cable.

the parasitic capacitances in the power cable may reduce the actual *LCL*-filter resonance to a lower value and even trigger multiple resonances [17]. Hence, the active damper is installed at the PCC of the inverter to suppress the resonances brought by the different system impedances.

B. Operation Principle

Fig. 2 illustrates the control diagram for the active damper. The active damper directly controls the resonant voltages at the PCC by means of multiple resonant controllers in parallel. Fig. 3 (a) shows the block diagram of the resonant controller based on two integrators, which can be expressed as

$$G_{rc,i}(s) = \frac{K_{r,i}\omega_{c,i}s}{s^2 + \omega_{c,i}s + \omega_{r,i}^2} \tag{1}$$

where ω_r and ω_c denote the center frequency and bandwidth of the resonant controller, respectively. To further improve the accuracy of the resonant controller in discretization, the sixth-order Taylor series approximation is used to correct the poles of the *z*-domain transfer function, as shown in Fig. 3 (b) [19].

It is worth noting that the active damper only works at the resonance frequencies, which is different from the APF for the steady-state harmonic compensation. The online detection of resonance frequencies is thus essential for the active damper to selectively control the resonant voltages. Although a number of harmonic estimation techniques are available [20], [21], the detection of multiple resonances is still a challenge in terms of computation burden and dynamic performance.

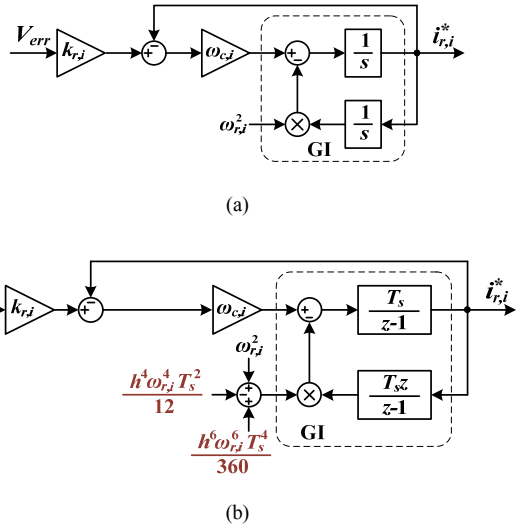

Fig. 3. Block diagram of the resonant controller based on two integrators. (a) Continuous form. (b) Discretized in *z*-domain.

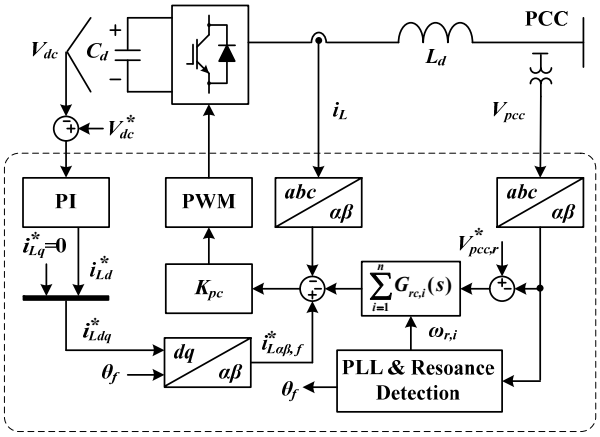

Fig. 2. Control bock diagram of the active damper.

III. Detection of Resonance Frequencies

This section first reviews the main types of ANF-based Phase-Locked Loop (PLL) or FLL for harmonic detection, and then proposes a cascaded ANF structure for the active damper based on the use of multiple ANFs and FLLs.

A. Overview of ANF-Based PLL/FLL

Fig. 4 depicts the block diagram representations for the 1-weight and 2-weight ANFs based on the Least Mean Square (LMS) adaptation algorithm [22], [23]. The LMS-based ANF was originally introduced for Active Noise Cancelling (ANC), which was later applied to improve the phase detection of PLL and developed a series of ANF-based PLL and FLL to retrieve sinusoidal signals in noises [24]-[35].

Fig. 5 shows the PLL based on the 1-weight ANF, which was first reported as the residual mode PLL [24], and then was developed as the Magnitude PLL (MPPL) for communication

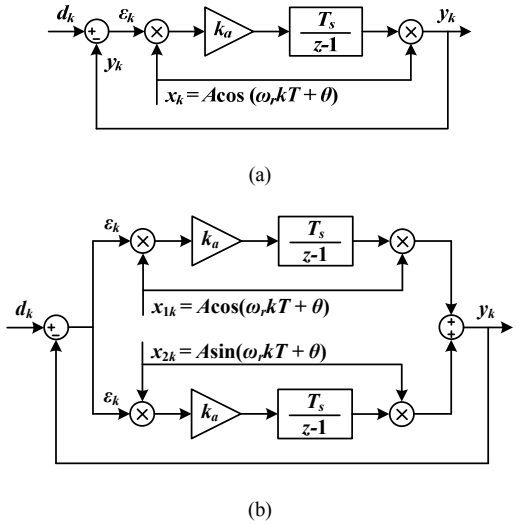

Fig. 4. Block diagrams for (a) 1-weight ANF, and (b) 2-weight ANF based on the LMS adaptation algorithm.

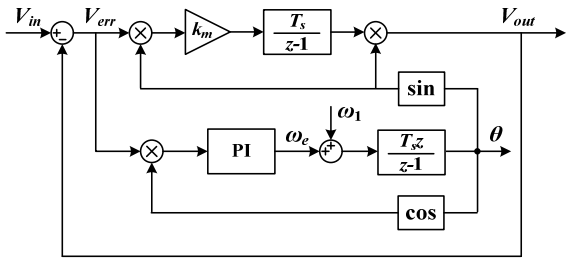

Fig. 5. The 1-weight ANF-based PLL structure.

systems [25]-[27], and the Enhanced PLL (EPLL) for power system frequency/phase tracking [28], [29]. Compared to the mixer phase detector, the ANF effectively reduces the second-order harmonics ripple. It has recently been found that several alternative single-phase PLLs have the same principle as the ANF-based PLL [30].

The similar application of the 2-weight ANF for PLL can be found in the Quadrature PLL (QPLL) [31]. Further, due to the equivalence between the continuous forms of the 2-weight ANF and the Generalized Integrator (GI) in Fig. 3, the ANF-based FLLs are developed based on the use of the generalized integrators [32]-[35]. Fig. 6 shows the block diagram of two ANF-based FLLs, where the ANF-based FLL in Fig. 6 (b) is also known as the Second-Order Generalized Integrator FLL (SOGI-FLL) [33]. It is interesting to see that the FLL in Fig. 6 employs the same phase detector as the PLL in Fig. 5, i.e. the product of the error signal and the quadrature signal.

B. Cascaded ANF Structure

The use of the multiple ANF-based PLL/FLL for harmonic estimation has been reported in [26], [34], where the parallel ANF structure is employed, as depicted in Fig. 7. This method works well for the detection of harmonic disturbances that are correlated to the fundamental frequency signal. However, its performance is deteriorated by the presence of interharmonics

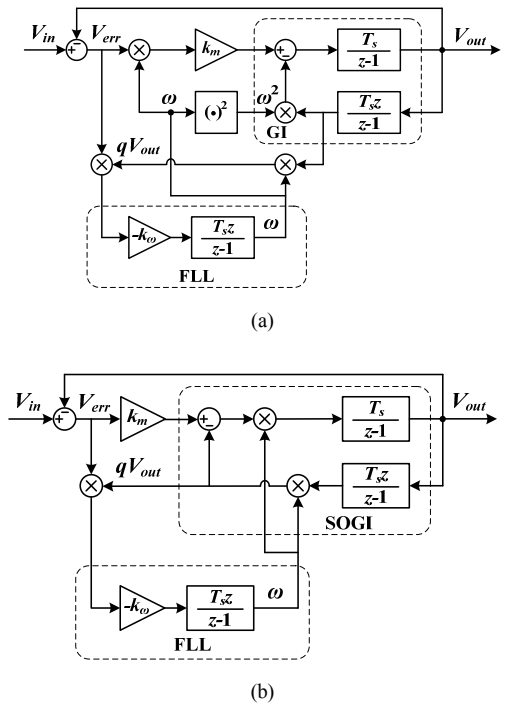

Fig. 6. 2-weight ANF-based FLLs. (a) ANF-based FLL with the generalized integrator. (b) SOGI-FLL.

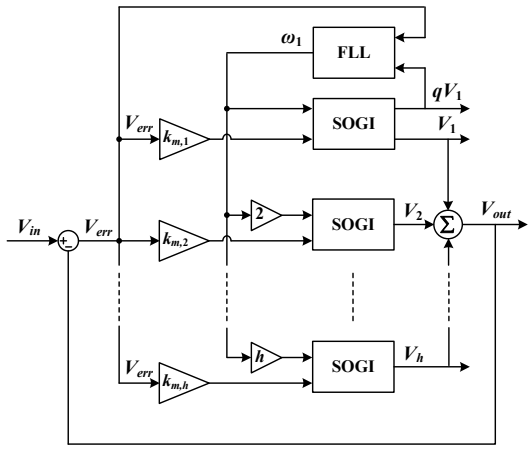

Fig. 7. Parallel ANF structure with a common FLL for harmonic detection.

or resonances [27], [35]. Therefore, to detect the resonances, a cascaded ANF structure is introduced in the following.

Fig. 8 shows the proposed cascaded ANF structure for the detection of resonance frequencies. Different from the parallel ANF structure with a common FLL in Fig. 7, multiple ANF-based FLLs are connected in cascade. Further, to decouple the harmonics or interharmonics disturbances near the resonance frequency, the Pre-filtered-ANF (P-ANF) structure is adopted [35]. Also, instead of the SOGI depicted in Fig. 6 (b), the ANF structure in Fig. 6 (a) is used, in order that the accuracy can be improved by using the GI in Fig. 3 (b).

Fig. 9 depicts the detection of resonances by the cascaded

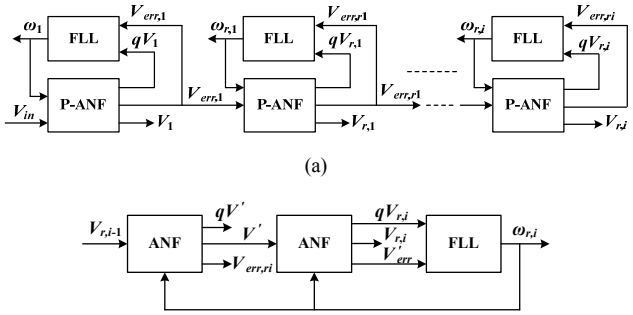

(a)

(b)

Fig. 8. Proposed cascaded ANF structure with multiple ANF-based FLLs. (a) Overall structure. (b) Pre-filtered-ANF (P-ANF).

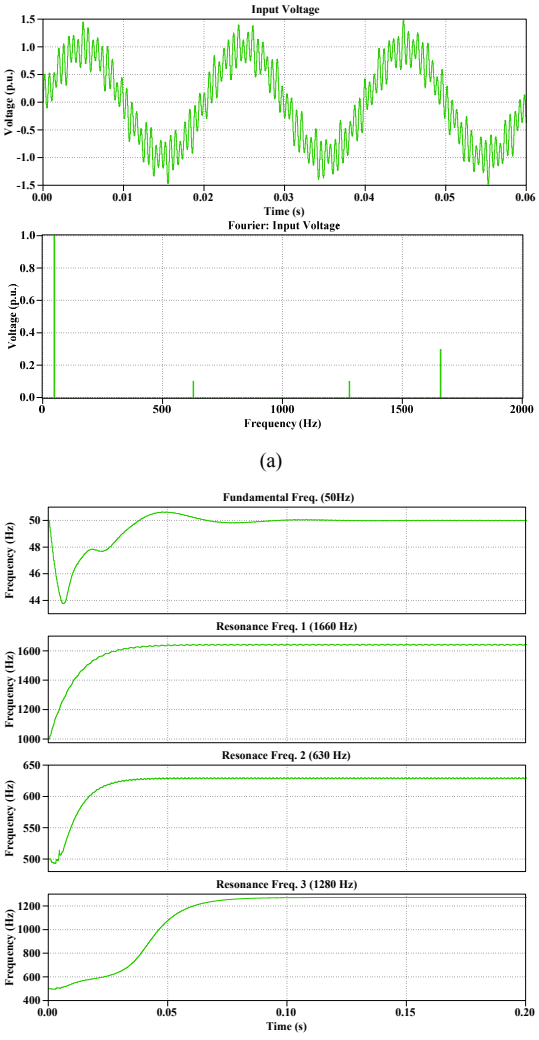

(a)

(b)

Fig. 9. Performance of the cascaded ANF structure for detecting multiple resonances. (a) Input voltage waveform and harmonic spectra. (b) Measured fundamental and resonance frequencies.

ANF structure. The input voltage signal is disturbed with three resonances at 1660 Hz, 630 Hz, and 1280 Hz, respectively. In three-phase systems, due to the presence of negative-sequence components, the positive-/negative-sequence calculation block needs to be used [34].

IV. Frequency-Domain Analysis

Fig. 10 depicts the current control loop for grid-connected inverter, where the main parameters are given in Tables I. The Proportional Resonant (PR) current controller in the stationary $\alpha\beta$-frame is adopted for the zero steady state error. Since the resonance frequency of *LCL*-filter is designed higher than the one-sixth of the control sampling frequency, there is no active damping loop. Further, to see the effect of the power cable and the grid impedance, the open-loop gains of the current control loop are derived as follows

$$T_c(s) = \frac{Z_{Cf} G_c G_d}{Z_{Lf} Z_{Cf} + Z_{Lf} Z_{Lg} + Z_{Cf} Z_{Lg}} \tag{2}$$

$$T_{ce}(s) = \frac{Z_{Cf} G_c G_d}{Z_{Lf} Z_{Cf} + Z_{Lf} (Z_{Lg} + Z_{eq}) + Z_{Cf} (Z_{Lg} + Z_{eq})} \tag{3}$$

where $T_c(s)$ and $T_{ce}(s)$ are the loop gains with and without the equivalent system impedance at the PCC, respectively. $G_c(s)$ is the PR current controller, and $G_d(s)$ is the computation and pulse width modulation delay involved in the digital control system. $Z_{eq}(s)$ represents the equivalent system impedance of inverter derived from the PCC.

Fig. 11 compares the frequency responses of the *LCL*-filter plant with and without the equivalent system impedance at the PCC. It is evident that the parasitic capacitances of the power cable introduce multiple resonance peaks into the plant of the current control loop. Correspondingly, a comparison of the frequency responses for the current control loop gain is shown in Fig. 12. Based on the Nyquist stability criterion, it can be found that one resonance peak that is lower than the one-sixth of the control sampling frequency leads to instability in the current control loop.

TABLE I. System Electrical Parameters

Parameters	Symbol	Value
Grid votlage	V_s	400 V/50 Hz
Grid inductance	L_s	1.5 mH
Cable inductance per section	L_l	1.5 mH
Cable resistance per section	r_l	0.075 Ω
Cable capacitance per section	C_l	4.7 μF
LCL-filter inductor (grid-side)	L_g	1.8 mH
LCL-filter capacitor	C_f	4.7 μF
LCL-filter inductor (inverter-side)	L_f	3 mH
Inverter switching frequency	f_{sw}	10 kHz
Filter inductor of active damper	L_d	3 mH
Active damper switching frequency	f_{swd}	20 kHz

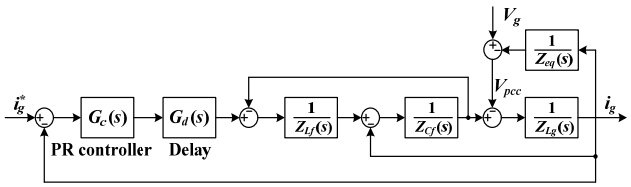

Fig. 10. Block diagram for the current control loop of grid-connected inverter.

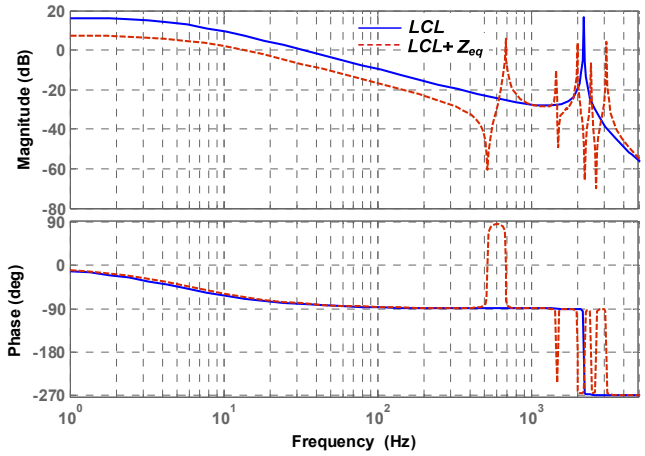

Fig. 11. Comparison of frequency responses of the *LCL*-filter plant with and without the equivalent system impedance at the PCC.

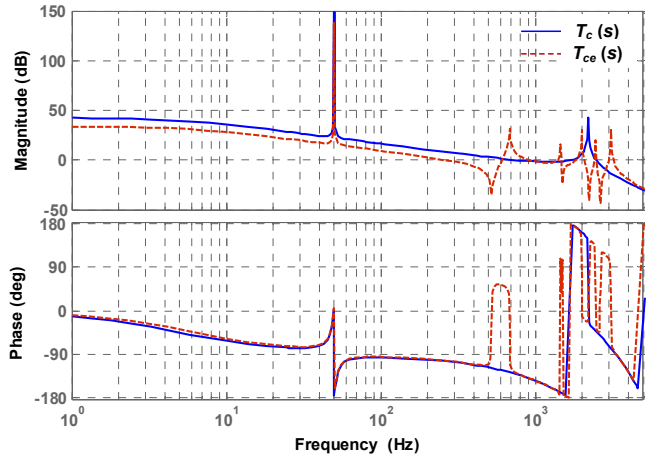

Fig. 12. Comparison of frequency responses of the open-loop gain of current control loop with and without the equivalent system impedance at the PCC.

From Fig. 12, it is known that the current control loop is unstable due to the resonance peak closed to 1520 Hz. Hence, the active damper has to be enabled to suppress the resonance. Fig. 13 depicts the effect of the active damper in the frequency domain. Notice that the active damper can be represented by the resonant voltage controllers expressed in (1), where the gains of the resonant controllers are equal to the reciprocal of equivalent resistances provided by the active damper [15]. It is seen that the unstable resonance peak can be damped by the active damper.

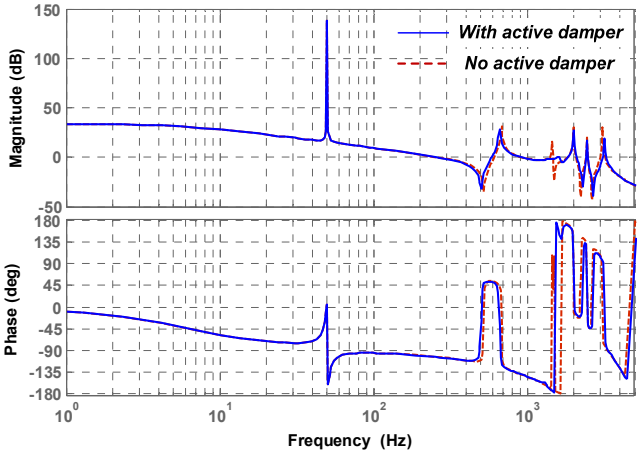

Fig. 13. Effect of active damper in the frequency domain.

V. Simulation Results

To further validate the performance of the active damper, the nonlinear time domain simulations for the system shown in Fig. 1 are carried out in MATLAB/SIMULINK and PLECS Blockset. The parameters listed in Table I are adopted for the simulation model.

First, to see the effect of the power cable on the stability of the current control loop, Fig. 14 shows the simulated voltage and current waveforms of the grid-connected inverter without enabling the active damper. The inverter is switched from the ideal AC voltage source to the power cable at the time instant of 0.2 s. It can be seen that the inverter becomes unstable due to the parasitic capacitances in the power cable, which further validate the frequency domain analysis depicted in Fig. 12. The corresponding harmonic spectra for the resonant voltage and current are shown in Fig. 15. It is seen that two resonance peaks are triggered around 1520 Hz and 1620 Hz.

Fig. 16 shows simulated inverter current and PCC voltage after enabling the active damper. The inverter is also switched from the ideal AC voltage source to the power cable at the time instant of 0.2 s. It is clear that the inverter is stabilized by the active damper.

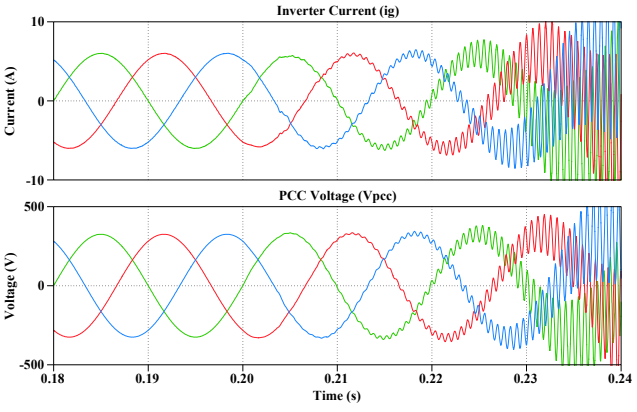

Fig. 14. Simulated inverter current and PCC voltage without enabling the active damper.

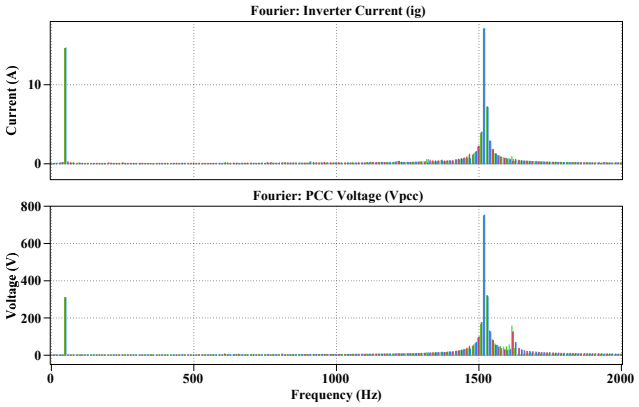

Fig. 15. Harmonic spectra for the resonant voltage and current in Fig. 14.

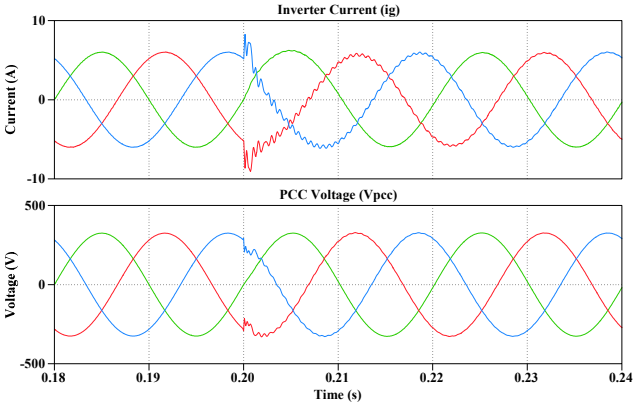

Fig. 16. Harmonic spectra for the resonant voltage and current in Fig. 14.

VI. CONCLUSIONS

This paper has introduced an active damper which can suppress multiple resonances with unknown frequencies. The active damper is based on a high-bandwidth power converter, which selectively control the resonant voltages at the PCC of the grid-connected inverter. Further, a cascaded ANF-based FLL structure has been discussed, which enables the active damper to estimate the frequencies of resonances, and thus realizing the frequency adaptive control for the resonances in the system. The cascaded ANF structure is different from the parallel ANF structure with a common FLL, since the latter normally used to detect the harmonics that are correlated to the fundamental frequency signal and is thus sensitive to the interharmonics or resonances at the input signals. In contrast, the cascaded ANF structure provides a way to retrieve the sinusoids in noises. Both the frequency domain analysis and time domain simulations have been presented to validate the performance of the active damper and the resonance frequency estimation method.

REFERENCES

[1] F. Blaabjerg, Z. Chen, and S. B. Kjaer, "Power electronics as efficient interface in dispersed power generation systems," *IEEE Trans. Power Electron*., vol. 19, no. 5, pp. 1184-1194, Sept. 2004.

[2] X. Wang, J. M. Guerrero, F. Blaabjerg, and Z. Chen, "A review of power electronics based microgrids," *Journal of Power Electron*., vol. 12, no. 1, pp. 181-192, Jan. 2012.

[3] Z. Shuai, D. Liu, J. Shen, C. Tu, Y. Cheng, and A. Luo, "Series and parallel resonance problem of wideband frequency harmonic and its elimination strategy," *IEEE Trans. Power Electron*., vol. 29, no. 4, pp. 1941-1952, Apr. 2014.

[4] M. Liserre, F. Blaabjerg, and S. Hansen, "Design and control of an *LCL*-filter-based three-phase active rectifier," *IEEE Trans. Ind. Appl*., vol. 41, no. 5, pp. 1281-1291, Sep./Oct. 2005.

[5] X. Wang, F. Blaabjerg, Z. Chen, and W. Wu, "Modeling and analysis of harmonic resonance in a power electronics based AC power system," in *Proc. IEEE ECCE* 2013, pp. 5529-5236.

[6] X. Wang, F. Blaabjerg, Z. Chen, and W. Wu, "Resoannce analysis in parallel voltage-controlled distributed generation inverters," in *Proc. IEEE APEC* 2013, pp. 2977-2983.

[7] F. Wang, J. L. Duarte, M. A. M. Hendrix, and P. F. Ribeiro, "Modeling and analysis of grid harmonic distortion impact of aggregated DG inverters," *IEEE Trans. Power Electron*., vol. 26, no. 3, pp. 786-797, Mar. 2011.

[8] S. Liang, Q. Hu, W. Lee, "A survey of harmonic emissions of a commecially operated wind farm," *IEEE Trans. Ind. Appl*., vol. 48, no. 3, pp. 1115-1123, May/Jun. 2012.

[9] J. Dannehl, M. Liserre, F. W. Fuchs, "Filter-based active damping of votlage source converters with *LCL* filter," *IEEE Trans. Ind. Electron*., vol. 58, no. 8, pp. 3623-3633, Aug. 2011.

[10] X. Wang, F. Blaabjerg, and Z. Chen, "Autonomous control of inverter-interfaced distributed generation units for harmonic current filtering and resonance damping in an islanded microgrid," *IEEE Trans. Ind. Appl*., Early Access Article, 2013.

[11] L. Harnefors, L. Zhang, and M. Bongiorno, "Frequency-domain passivity-based current controller design," *IET Power Electron.*, vol. 1, no. 4, pp. 455-465, Dec. 2008.

[12] T. Wang, Z. Ye, G. Sinha, and X. Yuan, "Output fitler design for a grid-interconnected three-phase inverter," in *Proc. IEEE APEC* 2003, vol. 2, pp. 779-784.

[13] M. Cespedes, L. Xing, and J. Sun, "Constant-power load system stabilization by passive damping," *IEEE Trans. Power Electron*., vol. 26, no. 7, pp. 1832-1836, Jul. 2011.

[14] R. N. Beres, X. Wang, F. Blaabjerg, M. Liserre, and C. L. Bak, "A review of passive filters for grid-connected voltage source converters," in *Proc. IEEE APEC* 2014, accepted.

[15] X. Wang, F. Blaabjerg, M. Liserre, Z. Chen, J. He, and Y. Li, "An active damper for stablizing power electronics based AC systems," *IEEE Trans. Power Electron*., Early Access Article, 2013.

[16] H. Akagi, H. Fujita, and K. Wada, "A shunt active filter based on voltage detection for harmonic termination of a radial power distribution line," *IEEE Trans. Ind. Appl.,* vol. 35, no. 3, pp. 638-645, May/Jun. 1999.

[17] S. Zhang, S. Jiang, X. Lu, B. Ge, and F. Z. Peng, "Resonance issues and damping techniques for grid-connected inverters with long transmission cable," *IEEE Trans. Power Electron*., vol. 29, no. 1, pp. 110-120, Jan. 2014.

[18] S. Parker, B. P. McGrath, and D. G. Holmes, "Region of active damping control for LCL filters," *IEEE Trans. Ind. Appl.*, Early Access Article, pp. 1-12, 2013.

[19] A. G. Yepes, F. Freijedo, O. Lopez, and J. Gandoy, "High-performance digital resonant controllers implemented with two integrators," *IEEE Trans. Power Electron*., vol. 26, no. 2, pp. 563-576, Feb. 2011.

[20] L. Asiminoaei, F. Blaabjerg, and S. Hansen, "Detection is key – harmonic detection methods for active power filter applications," *IEEE Ind. Appl. Mag.*, vol. 13, no. 4, pp. 22-33, Jul./Aug. 2007.

[21] E. Lavopa, P. Zanchetta, M. Sumner, and F. Cupertino, "Real-time estimation of fundamental frequency and harmonics for active shunt power filters in aircraft electrical systems," *IEEE Trans. Ind. Electron.,* vol. 56, no. 8, pp. 2875-2884, Aug. 2009.

[22] J. R. Glover Jr., "Adaptive noise canceling applied to sinusiodal interferences," *IEEE Trans. Acoust., Speech, Singal Process.,* vol. ASSP-25, no. 6, pp. 484-491, Dec. 1977.

[23] B. Widrow, J. R. Glover Jr., J. M. McCool, J. Kaunitz, C. S. Williams, R. H. Hearn, J. R. Zeidler, E. Dong Jr. and R. C. Googlin, "Adaptive noise canceling: principles and applications," in *Proc. IEEE*, vol. 73, no. 12, pp. 1692-1716, Dec. 1975.

[24] J. G. Mark, J. R. Steele, and C. C. Hansen, "Residual mode phase locked loop," U.S. Patent 4 495 475, Jan. 8, 1982.

[25] M. Bodson, "A discussion of Chaplin and Smith's Patent for the cancellation of repetitive vibrations," *IEEE Trans. Automat. Contr.,* vol. 44, no. 11, pp. 2221-2225, Nov. 1999.

[26] B. Wu and M. Bodson, "A magnitude/phase locked-loop approach to parameter estimation of periodic signals," *IEEE Trans. Automat. Contr.,* vol. 48, no. 4, pp. 612-618, Apr. 2003.

[27] X. Guo and M. Bodson, "Analysis and implementation of an adaptive algorithm for the rejection of multiple sinusoidal disturbances," *IEEE Trans. Control Syst. Technol.,* vol.17, no. 1, pp. 40-50, Jan. 2009.

[28] M. Karimi-Ghartemani and M. R. Iravani, "A nonlinear adaptive filter for on-line signal analysis in power systems: applications," *IEEE Trans. Power Del.,* vol. 17, no. 4, pp. 617-622, Apr. 2002.

[29] M. Karimi-Ghartemani and M. R. Iravani, "A method for synchronization of power electronic converters in polutted and variable-frequency environments," *IEEE Trans. Power Sys.,* vol. 19, no. 3, pp. 1263-1270, Aug. 2004.

[30] M. Karimi-Ghartemani, "A unifying approach to single-phase synchronous reference frame PLLs," *IEEE Trans. Power Electron*., vol. 28, no. 10, pp. 4550-4556, Oct. 2013.

[31] M. Karimi-Ghartemani, "A magnitude/phase-locked loop system based on estimation of frequency and in-phase/quadrature-phase applications," *IEEE Trans. Ind. Electron*., vol. 51, no. 2, pp. 511-517, Apr. 2004.

[32] M. Mojiri, M. Karimi-Ghartemani, and A. Bakhshai, "Estimation of power system frequency using adaptive notch filter," *IEEE Trans. Instrum. Meas.* vol. 56, no. 6, pp. 2470-2477, Dec. 2007.

[33] P. Rodriguez, A. Luna, R. S. Munoz-Aguilar, I. Qtadui, R. Teodorescu, and F. Blaabjerg, "A stationary reference frame grid synchronizaiton system for three-phase grid-connected power converters under adverse grid conditions," *IEEE Trans. Power Electron*., vol. 27, no. 1, pp. 99-112, Jan. 2012.

[34] P. Rodriguez, A. Luna, I. Candela, R. Mujal, R. Teodorescu, and F. Blaabjerg, "Multiresonant frequency-locked loop for grid synchronizaiton of power converters under distorted grid conditions," *IEEE Trans. Ind. Electron*., vol. 58, no. 1, pp. 127-138, Jan. 2011.

[35] J. Matas, M. Castilla, J. Miret, L. G. Vicuna, and R. Guzman, "An adaptive prefiltering method to improve the speed/accuracy tradeoff of voltage sequence detection methods under adverse grid conditions," *IEEE Trans. Ind. Electron*., vol. 61, no. 5, pp. 2139-2151, May 2014.